Journal of Medicinal Chemistry

Article

pubs.acs.org/jmc

From a Marine Neuropeptide to Antimicrobial Pseudopeptides Containing Aza-β^3-Amino Acids: Structure and Activity

Mathieu Laurencin,[†,∥] Baptiste Legrand,[‡,∥] Emilie Duval,[§] Joël Henry,[§] Michèle Baudy-Floc'h,*[,†] Céline Zatylny-Gaudin,[§] and Arnaud Bondon*[,‡]

[†]Université de Rennes 1, ICMV, UMR CNRS 6226, 263 Avenue du Général Leclerc, 35042 Rennes Cedex, France

[‡]Université de Rennes 1, CS 34317, Sim, UMR CNRS 6290, PRISM, Campus de Villejean, 35043 Rennes Cedex, France

[§]Université de Caen Basse Normandie, UMR 100 IFREMER PE2M, 14032 Caen Cedex, France

Supporting Information

ABSTRACT: Incorporation of aza-β^3-amino acids into an endogenous neuropeptide from mollusks (ALSGDAFLRF-NH_2) with weak antimicrobial activity allows the design of new AMPs sequences. Depending on the nature of the substitution, this can render the pseudopeptides inactive or lead to a drastic enhancement of the antimicrobial activity without high cytotoxicity. Structural studies of the pseudopeptides carried out by NMR and circular dichroism show the impact of aza-β^3-amino acids on peptide structure. The first three-dimensional structures of pseudopeptides containing aza-β^3-amino acids in aqueous micellar SDS were determined and demonstrate that the hydrazino turn can be formed in aqueous solution. Thus, AMP activity can be modulated through structural modifications induced by the nature and the position of such amino acid analogues in the peptide sequences.

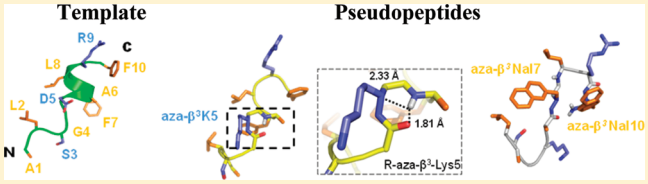

INTRODUCTION

Antimicrobial α-peptides (AMPs) are naturally occurring peptides that play an essential role in the host innate defense of wide array of organisms and are among the most important antibacterial agents.[1−5] Presently, databases contain over 1000 sequences for natural AMPs (http://www.bbcm.units.it/~tossi/amsdb.html), whereas several thousand have been designed de novo and produced synthetically.[6] Although they widely differ in sequence, AMPs are usually short (12−50 residues) and comprise hydrophobic and cationic residues, spatially segregated in amphipathic structures. Many AMPs kill microorganisms by permeabilization of the cytoplasmic membrane, whereas others penetrate into the cell and target additional anionic intracytoplasmic constituents (e.g., DNA, RNA, proteins, or cell wall components).[7] These modes of action require interaction with the cell membrane and numerous interaction models have been proposed including the barrel-stave pore,[2] the toroidal pore,[8] the carpet-like,[2] the aggregate,[9] and the detergent-like models.[10,11]

Because of the low degree of selectivity between microbial and host cells and the vulnerability of peptides to rapid in vivo degradation, AMPs have yet to see widespread clinical use.[3] A strategy to improve the activity, selectivity, and bioavailability of natural peptides is to design pseudopeptides. Recently, numerous peptide mimics have been developed including β-peptides,[12−14] peptoids,[15−17] β-peptoids,[18,19] and oligoureas.[20] Our present work concerns the antimicrobial properties of pseudopeptides containing aza-β^3-amino acids.

Aza-β^3-amino acids, in which the CH_β of a β^3-aminoacid is replaced by a nitrogen stereocenter atom, are known to enhance the bioavailability of biological active peptides, particularly in immunological applications.[21] This has been attributed to enhanced flexibility of the pseudopeptide arising from the side chain attached to the chiral nitrogen atom with nonfixed configuration.[22] These unnatural oligomers have an extended conformational space and are believed to adopt noncanonical secondary structures. To date, no structure of a peptide containing aza-β^3-amino acids has been determined in solution. X-ray crystal structures of linear and macrocyclic aza-β^3-peptides are known and exhibit an internal hydrogen-bond network leading to bifidic eight-membered ring pseudocycles, called N−N turns or hydrazino turns.[23−25] However, it was recently demonstrated that in the case of heteromacrocycles, inversion at the nitrogen center can be prevented by incorporating chiral monomers.[26]

Seawater contains many invasive microorganisms (up to 10^6 bacteria/mL and 10^9 virus/mL), and marine invertebrates have a large number of AMPs.[27] Some neuropeptides or peptidic hormones display structural similarities with AMPs and exhibit antimicrobial activities.[28] We have identified a short neuropeptide, H-ALSGDAFLRF-NH_2 (AD), of the cuttlefish *Sepia officinalis*, belonging to the FMRF-amide-related peptides (FaRPs), which is involved in the control of chromatophores and reproductive functions in cuttlefish.[27] This decapeptide has weak antimicrobial activity and a very low mammalian cell cytotoxicity and, therefore, is well suited as a template to study the impact of the incorporation of aza-β^3-amino acids on

Received: September 1, 2011
Published: February 9, 2012

Table 1. Antibacterial Activities of Peptides and Pseudopeptides Expressed As the Minimal Inhibitory Concentration (MIC, $\mu g \cdot mL^{-1}$)

	cuttlefish peptide	analogues of cuttlefish peptide					antibiotics
	AD	AK	Aβ^3K	K-2Nal7	K-1Nal	K-2Nal	ampicillin
Gram Positive							
Bacillus megaterium	640	80	na	80	**20**	80	20
Enterococcus faecalis	na[a]	na	na	>640	>640	>640	5
Listeria monocytogenes	na	na	na	80	**80**	160	5
Staphylococcus aureus	na	320	na	80	**20**	40	5
Gram Negative							
Escherichia coli	640	80	na	320	**40**	160	5
Salmonella typhimurium	na	320	na	80	**80**	160	5
Pseudomonas aeruginosa	na	640	>640	160	160	320	320
Klebsiella pneumoniae	na	>640	na	na	na	>640	5
Vibrio harveyi	>640	320	na	**40**	640	640	>320
Vibrio alginolyticus	320	320	na	**80**	>640	>640	>320
Vibrio aestuarianus	640	80	na	**40**	80	80	5
Vibrio splendidus	320	40	320	**20**	320	640	10

[a]na: not active.

antimicrobial activity. A large range of N^{β}-Fmoc-aza-β^3-amino acids with proteinogenic and nonproteinogenic side chains have been synthesized and incorporated into peptide sequences via solid-phase peptide synthesis (SPPS).[29−32] These peptides and pseudopeptides were tested on various Gram positive and Gram negative bacteria, including marine bacteria encountered by the cuttlefish and typical human pathogens. In addition, their structures were determined by NMR.

Substitutions of α-amino acids by aza-β^3-amino acids in this marine neuropeptide can induce a strong improvement or, conversely, lead to a complete loss of antimicrobial activity. Structural analysis of AD and AK (H-ALSGKAFLRF-NH_2) in SDS micelles indicated that the destabilization of the C-terminal amphiphilic helical moiety, induced by aza-β^3 residues, could explain the differences in antimicrobial activity. This permits to tentatively rationalize the structure−activity relationship of the studied peptides and pseudopeptides.

RESULTS AND DISCUSSION

Design of Antimicrobial Analogues. The neuropeptide AD possesses a net charge of +1 at physiological pH. Antimicrobial activity can often be improved by increasing the peptide net positive charge which creates stronger electrostatic interactions with the negatively charged bacterial membrane. Consequently, we first replaced the aspartic acid residue in position 5 by a lysine residue. The resulting peptide AK has the same hydrophobic ratio as AD, namely 50%, but possesses a net charge of +3 at physiological pH and an isoelectric point (pI) of 14 compared to 11 for AD. AK, in turn, was converted into four pseudopeptides containing standard α-amino acids or aza-β^3-amino acids. Substitution of α-amino acids by aza-β^3-amino acids relieves stereochemical constraints and may enhance proteolytic resistance.[21]

The pseudopeptide Aβ^3K (H-ALSG-aza-β^3-K-AFLRF-NH_2) was obtained from AK by replacing a lysine in position 5 by an aza-β^3-lysine. Substitution of one phenylalanine residue of AK by an aza-β^3-2-naphthylalanine provided K-2Nal7 (H-ALSG-KA-aza-β^3-2-Nal-LRF-NH_2), which displays good antimicrobial activity (Table 1). On the basis of this result, two new pseudopeptides, K-1Nal (H-ALSGKA-aza-β^3-1-Nal-LR-azaβ^3-1-Nal-NH_2) and K-2Nal (H-ALSGKA-aza-β^3-2-Nal-LR-aza-β^3-2-Nal-NH_2) were synthesized where both phenylalanine residues are replaced by aza-β^3-naphthylalanine. This mode of substitution has already been reported to improve antimicrobial activity of therapeutic potential.[33] Nevertheless, this improvement is very often coupled with a decrease in the cell selectivity[34,35] because synthetic peptides containing naphthylalanine amino acid are generally more hemolytic compared to the parent peptides. Indeed, this residue is known to enhance the interaction of AMPs with the lipid bilayers,[36] as the naphthyl nucleus, structurally close to the indole ring of tryptophan, is able to promote the AMPs burying within the hydrophobic core of the lipid bilayer.

Antibacterial Activity. The antibacterial activity of our pseudopeptides was assayed with a representative set of Gram positive and Gram negative bacteria (Table 1). The results allow us to compare the antibacterial activities of these analogues with the endogenous peptide AD. Ampicillin, a common antibiotic, served as the control. Neuropeptide AD possesses a narrow-spectrum antibacterial activity and acts more specifically on marine bacteria of the genus *Vibrio* but with relatively high MICs (>320 $\mu g \cdot mL^{-1}$). Indeed, its MICs are much higher than other marine antimicrobial peptides, so it is unlikely that AD is responsible for the cuttlefish's innate immunity. In contrast, the defensin MGD-1 of *Mytilus galloprovincialis* exhibits MICs that are 25−100 times lower.[37] AD's antibacterial properties may result from the close structural resemblance of this short neuropeptide with AMPs.

As expected, the simple D5 > K substitution considerably improves the antibacterial activity of the natural peptide. The peptide AK possesses a larger antibacterial spectrum than native AD. It is active against all the Gram negative bacteria tested as well as the Gram positive bateria *Staphylococcus aureus* and its MICs are significantly lowered compared to ADs, eight times lower for *Bacillus megaterium*, *Escherichia coli*, *Vibrio splendidus*, and *Vibrio aestuarianus*. In addition, marine bacteria are more affected by this peptide: a concentration of only 40 $\mu g \cdot mL^{-1}$ inhibits the growth of *V. splendidus*.

In contrast, substitution of the lysine in position 5 by an aza-β^3-amino acid leads to significant loss in antimicrobial activity; Aβ^3K is only active against *V. splendidus*. This demonstrates that the incorporation of an aza-β^3-amino acid can also switch off biological activity. It is interesting to note that the side chains are similar for AK and Aβ^3K, the loss of activity is solely due to

dx.doi.org/10.1021/jm2011595 | J. Med. Chem. 2012, 55, 2025−2034

a global fold modification arising from a change in the peptide backbone.

On the other hand, the three other pseudopeptide variations, K-2Nal7, K-1Nal, and K-2Nal, exhibit very broad antimicrobial spectra. They are active against the Gram positive bacteria *Enterococcus faecalis* and *Listeria monocytogenes*, whereas AK is not and are more than four times more effective against *S. aureus* than AK. An increase in activity against Gram negative nonmarine bacteria is also observed, particularly for *Salmonella typhimurium* and *Klebsiella pneumoniae*. With regard to the first eight bacterial strains in Table 1, K-1Nal possesses the lowest overall MICs with values of 20 $\mu g \cdot mL^{-1}$ for *B. megaterium* and *S. aureus* and 40 $\mu g \cdot mL^{-1}$ for *E. coli*. Surprisingly, K-2Nal, in which two isomeric aza-β^3-2-naphthylalanine residues are present, exhibits large variations in antimicrobial activity compared to K-1Nal. Its MICs either equal to or higher than those of K-1Nal. These results reveal the sensitivity of the interaction of the macrocycle with the bacterial walls. The antimicrobial activity of K-2Nal7 lies in between those of K-1Nal and K-2Nal. Finally, considering the four marine bacteria studied, K-1Nal and K2-Nal show similar antimicrobial activity to both AD and AK, whereas K-2Nal7 is the most effective, possessing the lowest MICs. In fact, K-2Nal7 is more effective against the *Vibrio harveyi* and *Vibrio alginolyticus* than ampicillin.

Hemolytic Activity and in Vitro Cytotoxicity of Analogues. Hemolytic activity and peptide cytotoxicity were measured on rabbit erythrocytes (Figure 1) and Chinese

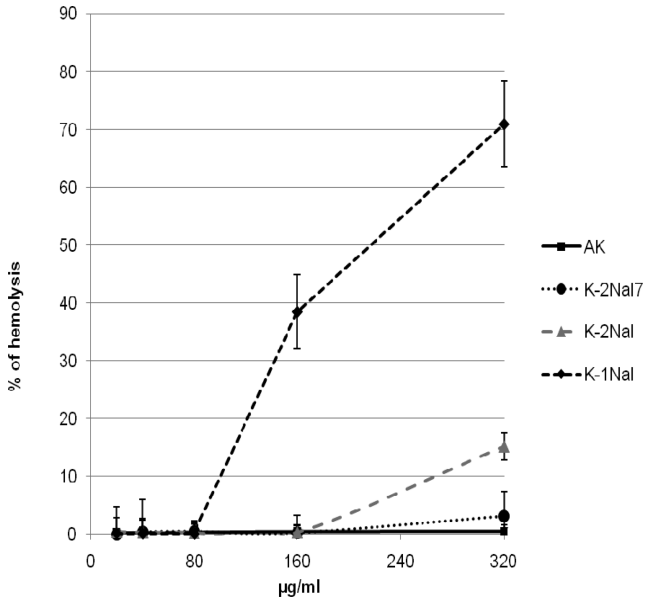

Figure 1. Hemolytic activities of pseudopeptides on rabbit erythrocytes.

hamster ovaries (*CHO-K1* cell line, Figure 2), respectively. AK displays no significant hemolytic activity (<1.5%) up to concentrations of 320 $\mu g \cdot mL^{-1}$. Its cytotoxicity is also very low, 640 $\mu g \cdot mL^{-1}$, with 87% viability, which indicates good selectivity for bacterial cells over mammalian cells. The pseudopeptide K-1Nal, however, is hemolytic; a 50% hemolytic dose (HD_{50}) close to 200 $\mu g \cdot mL^{-1}$ was measured. This is lower than some MICs but 10 times higher than MIC measured for the pathogen *S. aureus*. K-2Nal is less hemolytic than K-1Nal, causing only 14% of hemolysis at 320 $\mu g \cdot mL^{-1}$. Concerning the

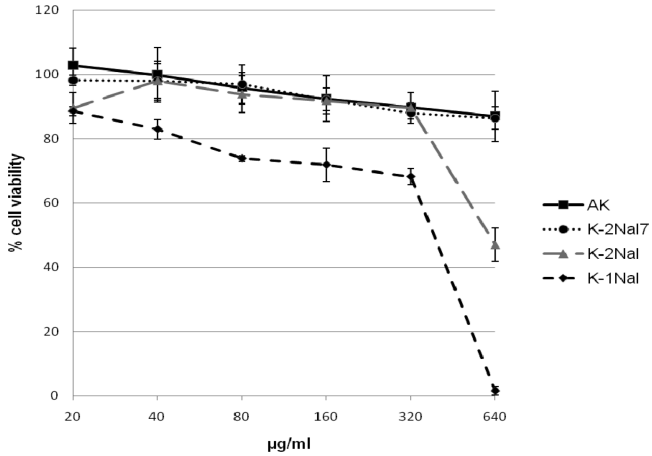

Figure 2. Cytotoxic activities of pseudopeptides on Chinese hamster ovarian cells (CHO-K1 cell line).

cytotoxicity, at a concentration of K-2Nal of 640 $\mu g \cdot mL^{-1}$, a cell viability of 47% was measured. In contrast, K-1Nal appears to be highly toxic. Whereas small doses up to 40 $\mu g \cdot mL^{-1}$ are not cytotoxic to CHO-K1 cells, it is slightly cytotoxic at 160 $\mu g \cdot mL^{-1}$ (78% of viability) and toxic at 640 $\mu g \cdot mL^{-1}$. However, this latter concentration is 8 times higher than its MICs against human pathogens *L. monocytogenes* and *Salmonella typhimurium* and 32 times higher than its MIC against *S. aureus*. As often observed, the improvement of the antimicrobial activity is associated with a decline in the selectivity between prokaryotic and eukaryotic cells. The presence of the nonproteinogenic naphthylalanine side chains seems to decrease the peptide selectivity,[35] and the notable differences between K-1Nal and K-2Nal demonstrate that physicochemical parameters such as the orientation of the aromatic naphthylalanine moieties have a great influence on biological activity and selectivity. It is worthy to note that K-2Nal7, which contains one naphthylalanine side chain, displays only very weak hemolysis (5% at 320 $\mu g \cdot mL^{-1}$) or cytotoxicity (87% of viability at 640 $\mu g \cdot mL^{-1}$). These values are very similar to those of the α-peptide AK and indicate that naphthylalanine residue does not induce a decrease in systematic cell selectivity.

Circular Dichroism Analysis. The CD spectra of the endogenous peptide AD and its analogue AK are similar, in agreement with the adoption of identical structures in several media (Figure 3A). A random coil CD profile is obtained for both in phosphate buffer (10 mM KP, pH 7.4) and a typical helical signature in hydrophobic environments. Indeed, in 50% TFE or in the presence of SDS micelles, two media that mimic lipid membranes, their CD spectra exhibit a maximum at 190 nm and two minima around 208 and 222 nm, indicating that they adopt a well-defined helical character to some extent. Nevertheless, such short peptides (10 residues) cannot form more than one or two helical turns (3.6 residues per turn).

Interestingly, Aβ^3K displays a random profile in phosphate buffer but an atypical CD profile in the presence of SDS micelles with a thin minimum at 202 nm (Figure 3B), attributable to the presence of turns within the peptidic backbone. The lack of the activity of Aβ^3K may, therefore, be caused by the loss of helicity due to the incorporation of the aza-β^3-K in position 5. K-2Nal7 exhibits a similar profile to that of Aβ^3K, i.e., no helical conformation can be detected (Figure 3B). In the case of pseudopeptides K-1Nal and K-2Nal (Figure 3C,D), interpretation of the CD spectra is difficult due to the

dx.doi.org/10.1021/jm2011595 | J. Med. Chem. 2012, 55, 2025−2034

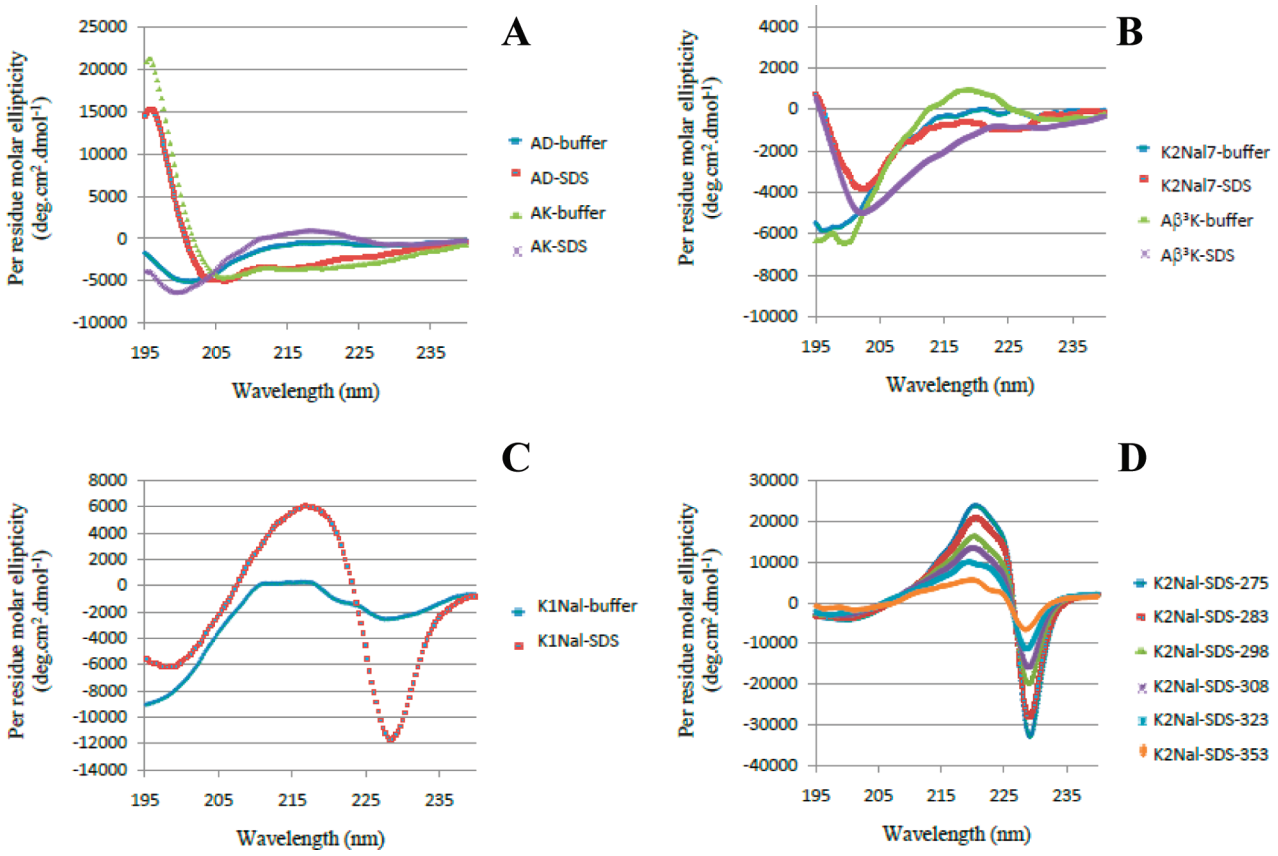

Figure 3. CD spectra of AD and AK (A), Aβ^3K and K-2Nal7 (B), K-1Nal (C), and temperature dependence of K-2Nal (D). Buffer, 10 mM phosphate buffer; SDS, 30 mM SDS in buffer.

strong absorbance of the aromatic nuclei of aza-β^3-naphthylalanine residues. Nevertheless, it is clear that they adopt a random coil conformation in phosphate buffer. Dramatic changes occur in 50% TFE and especially in the presence of SDS micelles where K-1Nal exhibits a couplet centered at 223 nm with a maximum at 217 nm and a minimum at 228 nm. The spectrum of K-2Nal exhibits the same pattern, but its couplet is centered at 226 nm with a minimum at 221 nm and a maximum at 229 nm. From previous studies of poly(L-1-naphthyalanine) and poly(L-2-naphthyl alanine) peptides,[38,39] the signal centered around 225 nm can be attributed to the ^1B_b transition of naphthalene groups. Dathe and co-workers obtained the same type of CD profiles with the cyclic antimicrobial hexapeptide RNal (*cyclo*[-R-R-1Nal-1Nal-R-F-]) which also contains two α-L-naphthylalanine residues. In SDS micelles or POPG small unilamellar vesicles (SUVs),[34] RNa1 exhibits a CD spectrum displaying a couplet centered at 227 nm with a maximum at 222 nm and a minimum at 232 nm.[34] It is important to note that the couplet is inverted in the case of the antimicrobial D-peptide D-Nal-Pac-525 (*Ac*-k-nal-r-r-nal-v-r-nal-i-NH_2). In the presence of phospholipids or micelles, this peptide displays the same type of couplet centered at 225 nm but with the maximum at 229 nm and the minimum at 220 nm.[35]

In the case of our pseudopeptides, the two aza-β^3-naphthylalanine residues are separated by two residues along their long axis. Moreover, the aromatic side chains are bound to chiral nitrogen atoms without a fixed configuration, consistent with a distance between the aromatic residues short enough to allow dipole−dipole interaction. Thus, the CD spectra in SDS micelles seem to indicate that the side chains are preferentially positioned in an orientation similar to α-naphthylalanine with a L configuration (absolute configuration *S*). Furthermore, the CD spectra of K-2Nal in the presence of SDS micelles (reported in Figure 3D) show a strong temperature dependence, the intensity of the maxima and minima decreasing with increasing temperature. This must result from a change in distance between the naphthalene rings due to thermal motion or rapid inversion of the nitrogen stereochemistry.

NMR Experiments and Structure Calculations. Because the CD spectra revealed that the five peptides AD, AK, Aβ^3K, K-2Nal7, and K-2Nal, adopt specific conformations in presence of SDS micelles, NMR structural studies were performed in this same medium. In the case of Aβ^3K, K-2Nal7, and K-2Nal, where the aza-β^3-amino acids side chain are attached to an unprotonated nitrogen atom, no transfer of magnetization from the amidic proton can be seen in the TOCSY spectra. However, starting from the typical amide proton singlet for the aza-β^3-residue near 9 ppm, the side chain proton resonance of this residue can be easily identified in the NOESY spectra. The strong NOEs between H_α of the aza-β^3 residue and the amide proton of the precedent amino acid allowed assignment of the sequence as reported in the Supporting Information Table S1.

Where possible, NOEs are assigned based on unambiguous chemical shift assignments. However, due to overlap of certain signals, ambiguous NOEs are also used for the ARIA analysis. In the final ARIA run, the AD structure was calculated using 147 distance restraints and 5 dihedral restraints for the Leu2, Asp5, Ala6, Leu8, and Arg9 residues. In the last iteration, 60 structures were refined in a shell of water and the 20 lowest

dx.doi.org/10.1021/jm2011595 | *J. Med. Chem.* 2012, 55, 2025−2034

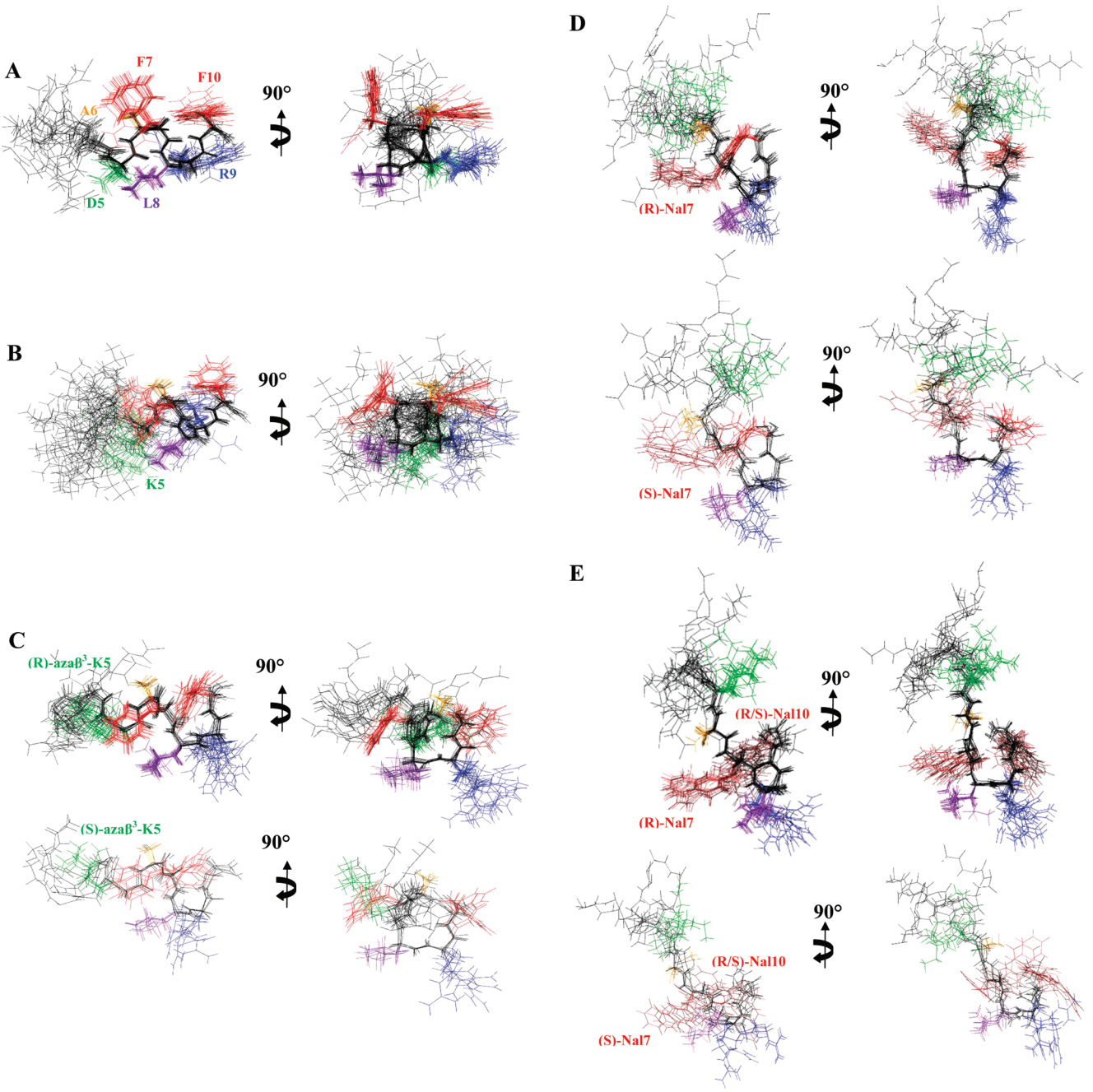

Figure 4. The 20 lowest energy structures with no violations >0.3 Å from the 60 structures calculated in the final iteration of ARIA for neuropeptide analogues in SDS micelles. (A) AD, (B) AK, (C) the two set of structures for Aβ^3K, (D) K-2Nal7, and (E) K-2Nal, corresponding to the two possible configurations of aza-β^3-lysine or aza-β^3-naphtylalanine moieties. The superposition was performed using the backbone atoms of residues 5−10. For clarity, the side chains of residues 1−4 are not drawn. The backbone of all structures is shown in black, while the side chains of the Phe residues are displayed in red, the Asp or Lys residues in green, the Ala residues in orange, the Leu residues in purple, and the Arg residue in blue.

energy conformers without distance violations >0.3 Å possessing good stereochemical quality are depicted in Figure 4. The global fold of AD in SDS micelles displays a disordered N-terminal domain and a well-defined helical encompassing residues 5 to 10. Indeed, the backbone rmsd for the whole structure is 1.312 Å and falls to 0.163 Å if the poorly defined N-terminus is ignored (see Supporting Information Table S2). This peculiarity is similar to structural features of other short neuropeptides belonging to the tachykinin family.[40] The AD structure is amphipathic (see Figure 4A). The polar residues Asp5 and Arg9 are aligned on one side of the helical turn, whereas a large hydrophobic surface composed of the Ala6, Phe7, Leu8, and Phe10 is on the other side. For the structure determination of AK, 170 distance restraints and five dihedral restraints (Lys5, Leu6, Phe7, Leu8, Arg9) were used in the final iteration of ARIA. The proton chemical shifts of AK are very close to those of AD and, as expected, the global folds of AK (Figure 4B) and AD are similar, possessing a disordered N-terminus and a well-defined helical turn from Lys5 to Phe10 (Figure 5). Thus, the structural effect of the mutation D5K on the neuropeptide is very slight and does not alter its amphipathicity.

dx.doi.org/10.1021/jm2011595 | J. Med. Chem. 2012, 55, 2025−2034

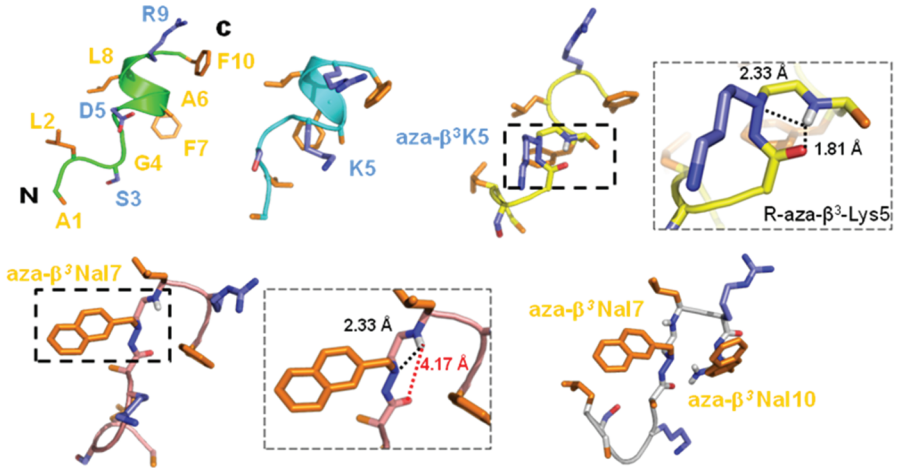

Figure 5. The best lowest energy structures of AD (green), AK (cyan), Aβ^3K (yellow), K-2Nal7 (pink), and K-2Nal (gray). The side chains of the polar and hydrophobic residues are in blue and orange, respectively. Aza-β^3 residue snapshots are available for the Aβ^3K and K-2Nal7 peptides (see also Supporting Information Table S2).

NMR analysis shows that the solution structure of Aβ^3K is clearly different than that of both AD and AK. As the stereochemistry of the nitrogen bearing the side chain of the aza-β^3 residue is not fixed, the configuration of the stereocenter of the aza-β^3-Lys5 is thus not specified in our dedicated CNS topology and parameter files. Therefore, the final restraint file of Aβ^3K comprises 213 distance restraints and three dihedral restraints. Despite a unique set of signals, two conformations according to the configuration *R* or *S* of the N^{α} stereocenter of the aza-β^3-Lys5 are among the 20 lowest energy structures, namely 15 with a *R* and 5 with a *S* configuration. The Aβ^3K NOESY spectrum exhibits 20% more NOE peaks than that of AD or AK because its backbone is quite well-defined all along the sequence (Figures 4 and 5). Moreover, in contrast to AK and AD, its global fold is very different and does not exhibit helical character. As can be seen in Figure 6, the introduction of the aza-β^3-Lys residue induces a hydrazino or N−N turn which has previously been observed in $CDCl_3$ and detected in aza-β^3-peptide crystal structures.[23−25] The amide proton of Leu6 forms a hydrogen bond with both the lone pair of the sp^3 nitrogen atom of the aza-β^3-Lys5 (6.HN-5.N$^{\alpha}$ = 2.33 Å) and the carbonyl of Gly4 (6.HN-4.CO = 1.81 Å). The four characteristic torsional angles, ω, φ, θ, and ψ, for the *R*- and the *S*-hydrazino turn have also been measured (Supporting Information, Table S3). Interestingly, this particular turn is surrounded by two β-turns composed of the residues 2−5 on the one side and 5−8 on the other side of the hydrazino turn (Figure 6), the former stabilized by hydrogen bonding between the carbonyl of Leu2 and amide protons of Gly4 (2.O−4.HN = 1.83 Å) and aza-β^3-Lys5 (2.O−5.HN = 2.31 Å) and the latter by hydrogen bonding between the carbonyl of aza-β^3-Lys5 and amide protons of Phe7 (5.O−7.HN = 1.82 Å) and Leu8 (5.O−8.HN = 2.33 Å). This specific folding feature is particularly stable and gives rise to the strong NOE peaks between the amide protons 2.HN−3.HN, 4.HN−5.HN, 7.HN−8.HN, and 9.HN−10.HN detected in the NOESY spectrum.

To our knowledge, this work describes the first three-dimensional structure determination of pseudopeptides containing aza-β^3-residues in an aqueous medium by NMR. The proposal of sets of structures with the *R* and *S* configurations of aza-β^3-lysine does not necessary mean that they are present in solution but rather that the distance restraints used in the NMR

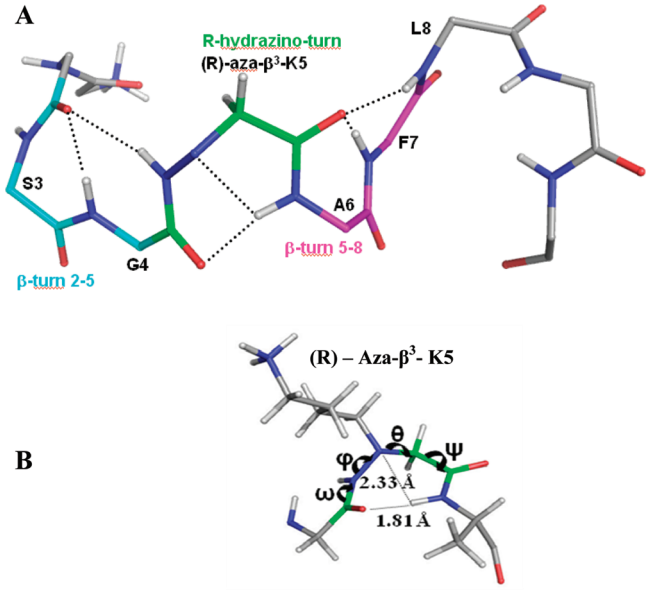

Figure 6. (A) Structural features of Aβ^3K. The carbon atoms of the *R*-hydrazino turn are displayed in green, and the two surrounding β-turn carbon atoms involving residues 2−5 and 5−8 in cyan and magenta, respectively. The side chains have been removed for clarity. Hydrogen bonds are represented with dashed lines. (B) Distances and torsion angles in the hydrazino turn.

structure calculations can be satisfied by the either the *R* or *S* configuration.

The incorporation of only one aza-β^3-residue dramatically modifies the well-ordered helices of AD and AK and induces a loss of the amphipathic properties which seems to be associated with antimicrobial activity. In K-2Nal7 and K-2Nal, only the C-termini are ordered and form β-turns which are in proximity to the hydrophobic aromatic residues in position 7 and 10 (Figure 4D,E). The distance between the aromatic rings, however, is too large to allow their interactions (~9 Å). Indeed, the NOEs of the pseudopeptides K-2Nal7 and K-2Nal in SDS micelles are generally lower than those of the three other peptides, indicating enhanced flexibility. It is, therefore, not surprising that the NOE observed for Aβ^3K NOESY, indicative for a hydazino turn, cannot be detected for K-2Nal7 and K-2Nal.

dx.doi.org/10.1021/jm2011595 | *J. Med. Chem.* 2012, 55, 2025−2034

In general, structural characterization of α-peptides and pseudopeptides allows the study the influence of the aza-β^3 residue. D5K substitution of the native peptide does not cause any loss of helicity, and the amphipathic character is conserved. Each introduction of aza-β^3 residues causes drastic structural changes, especially in the case of Aβ^3K having a well-defined and rigid backbone structure. Apparently, this rigidity is related to the disappearance of all antibacterial activity. When aza-β^3-naphthylalanine is introduced, only the C-terminal moieties are well-defined and adopt a β-turn, whereas the remainder of the peptide displays large flexibility. This flexibility, as well as the properties associated with the hydrophobic naphthylalanine side chain (higher absolute lipophilicity), induces an increase in antimicrobial activity.

This observation is consistent with the hypothesis that a helical structure is not necessary and that an increase in structural flexibility allowing the formation of an amphipathic structure could improve antimicrobial activity profile.[41−43] Such a conclusion has been reported in the case of various pseudopeptides containing β-amino acids as recently reviewed.[44] For example, mixed α/β peptides designed as a scrambled negative control (not able to adopt amphiphilic helical conformation) were shown to display good antimicrobial activities with MIC below 15 μg/mL against four bacterial strains and low hemolytic activities.[14,45] Interestingly, it was pointed out that flexibility and hydrophilic/lipophilic balance is more important that structural conformation.[45] In agreement with these findings, our mixed α/aza-β^3-pseudopeptides confirmed that formation of a globally amphiphilic helix is *not* required for host-defense peptide mimicry.

CONCLUSION

This article reports the first observation of antibacterial activity for a modified marine invertebrate neuropeptide. CD and NMR data show that the peptide AD adopts an amphiphilic α-helical conformation in hydrophobic medium, as seen for the majority of natural antimicrobial peptides. The importance of cationic net charge is demonstrated by the improvement of the antibacterial activity through simple substitution of aspartic acid to lysine to provide AK, which has no effect on peptide secondary structure. On the other hand, the incorporation of only one aza-β^3-amino acid can lead to a drastic rearrangement of the peptidic backbone, resulting in a rigid structure and the loss of antibacterial activity. This could be substantiated by the first three-dimensional structure determination of pseudopeptides with such aza-β^3-amino acid residues in an aqueous micellar environment. Interestingly, the three more biologically active pseudopeptides, K-2Na17, K-1Nal, and K-2Na1, display strong amphipathic character but do not possess helical structure.

As recently reported for heterogeneous helical urea/amide backbones[46] or mixed α/β peptides,[45] the introduction of aza-β^3-amino acids into peptides appears to be a promising strategy to fight multiresistant bacteria. This present work demonstrates that the position and number of aza-β^3-amino acid residues has a marked effect on structure and, in turn, biological activity.

EXPERIMENTAL SECTION

Peptides and Pseudopeptides Synthesis. Peptides (AD and AK) and the pseudopeptide Aβ^3K were synthesized on an Advanced Chem Tech 440 Mos synthesizer. Pseudopeptides K-2Nal7, K-1Nal, and K-2Nal were synthesized on a Pioneer peptide synthesis system. Synthesis was accomplished using commercially available N^{α}-Fmoc-amino acid, N^{β}-Fmoc-aza-β^3-amino acid,[29−32] and a Rink amide resin. Peptides were synthesized via Fmoc solid phase synthesis methods using a 4-fold excess of amino acid, TBTU, and HOBt in the presence of a 8-fold excess of DIPEA for 1 h for standard residues and 2 h for aza-β^3 residues. The Fmoc group was removed with 20% piperidine in DMF for 10 min. At the end of the synthesis, the resin was washed with CH_2Cl_2 and dried. Side chain deprotection and cleavage of peptides from the resin were performed simultaneously by treatment with TFA/H_2O/TIS (95/2.5/2.5, v/v/v) for 3 h. After filtration of the resin, the TFA solutions were concentrated in vacuo and peptides were precipitated by addition of cold diethyl ether. Peptides were purified by RP-HPLC on a C18 XTerra semipreparative column (10 μm, 19 mm × 300 mm, Waters) with a linear gradient of water, 0.08% TFA (A)/acetonitrile, 1% TFA (B) (5−60% B in 40 min and 60−100% B in 20 min, 8 mL/min, 215 nm) to a final purity of ≥95% and lyophilized. Characterization of purified peptides by RP-HPLC analyses were performed on a C18 XTerra (4.6 mm × 250 mm, 5 μm) column using water 0.08% TFA (A)/acetonitrile, 1% TFA (B) linear gradient (5−60% B in 20 min, 1 mL/min, 30 °C, 215 nm). Peptide concentrations for all experiments were calculated as the TFA salt (assuming association of one molecule of TFA per cationic residue, determined by ^{13}C NMR).

H-ALSGDAFLRF-NH_2 (AD): Yield after purification 26%; white powder; RP-HPLC t_R, 17.30 min; LC-ESI-MS/MS mass, m/z found 1095.27 [M + H$^+$]; calcd, 1095.59 [M + H$^+$].

H-ALSGKAFLRF-NH_2 (AK): Yield after purification 40%; white powder; RP-HPLC t_R, 16.93 min; LC-ESI-MS/MS mass, m/z found 1108.60 [M + H$^+$]; calcd, 1108.66 [M + H$^+$].

H-ALSG-**aza-β^3-K**-AFLRF-NH_2 (Aβ^3K): Yield after purification 18%; white powder; RP-HPLC t_R, 15.17 min; LC-ESI-MS/MS mass, m/z found 1123.65 [M + H$^+$]; calcd, 1123.67 [M + H$^+$].

H-ALSGKA-**aza-β^3-2Nal**-LRF-NH_2 (K2-Nal7): Yield after purification 58%; white powder; RP-HPLC t_R, 14.85 min; LC-ESI-MS/MS mass, m/z found 1173.70 [M + H$^+$]; calcd, 1173.69 [M + H$^+$].

H-ALSGKA-**aza-β^3-1Nal**-LR-**aza-β^3-1Nal**-NH_2 (K1-Nal): Yield after purification 21%; white powder; RP-HPLC t_R, 19.13 min; LC-ESI-MS/MS mass, m/z found 1238.65 [M + H$^+$]; calcd, 1238.71 [M + H$^+$].

H-ALSGKA-**aza-β^3-2Nal**-LR-**aza-β^3-2Nal**-NH_2 (K2-Nal): Yield after purification 55%; white powder; RP-HPLC t_R, 20.56 min; LC-ESI-MS/MS mass, m/z found 1238.65 [M + H$^+$]; calcd, 1238.71 [M + H$^+$].

Antibacterial Assays. The antibacterial activity of peptides was measured by liquid growth inhibition assay, performed in 96-well microtiter plates.[47] Microbial growth was assessed by measurement of the optical density at D_{595} after the 20 h incubation at 30 or 18 °C for *Vibrios*. The minimal inhibitory concentration (MIC) is defined as the lowest concentration required to inhibite growth (100% inhibition). The bacteria species tested were the Gram positive *Bacillus megaterium*, *Enterococcus faecalis*, *Listeria monocytogenes*, *Staphylococcus aureus*, and the Gram negative *Escherichia coli*, *Klebsiella pneumoniae*, *Pseudomonas aeruginosa*, *Salmonella typhimurium*, and marine *Vibrio*, (*V. aestuarianus*, *V. alginolyticus*, *V. harveyi*, and *V. splendidus*). For antibacterial tests, distilled water is used to dissolve peptides. Briefly, 10 μL of water or 10 μL of peptide solution at a final concentration ranging from 20 to 640 μg·mL^{-1} were incubated with 100 μL of a midlogarithmic growth phase culture of bacteria at a starting optical density of D_{600} = 0.001. Poor-broth nutrient medium (PB: 1% peptone, 0.5% NaCl, w/v, pH 7.5) was used for standard bacterial culture. Pathogenic bacteria were grown in PB with 0.3% of beef extract (BD) or in brain heart infusion for *Enterococcus* and *Listeria*. *Vibrios* were grown in saline PB (SPB: 1% peptone, 1.5% NaCl, w/v, pH 7.2).

Cytotoxicity Assay. Cytotoxicity of peptides on CHO-K1 cells was determined by the colorimetric MTT (3-[4,5-dimethylthiozol-2-yl]-2,5-diphenyltetrazolium bromide) dye reduction assay. Briefly, 1.34 × 10^4 cells/well in Ham F12 supplemented with L-glutamine (Gibco) and 10% fetal calf serum (Eurobio) were placed into 96-well plates. After incubation for 6 h under a fully humidified atmosphere of 95% room air and 5% CO_2 at 37 °C, analogues dissolved in phosphate

buffered saline (PBS) were added to cell cultures at a final concentration ranging from 20 to 640 $\mu g \cdot mL^{-1}$. After 36 h incubation, toxicity was evaluated by measuring the optical density of the culture at 570 nm using the cell growth determination kit (Sigma) based on conversion of the yellow tetrazolium salt MTT into purple formazan crystals by metabolically active cells. Finally, 100% of viability and 0% of viability were determined in PBS buffer and 1% Triton X-100, respectively. The experiments were set in triplicate.

Hemolytic Activity. The hemolytic activity of analogues was determined with freshly isolated rabbit erythrocytes as already described.[48] Erythrocytes solution was incubated for 1 h at 37 °C with peptide dissolved in PBS to reach 20 at 320 $\mu g \cdot mL^{-1}$. Hemolysis was determined by measuring the optical density of the supernatant at 415 nm. Zero hemolysis (blank) and 100% hemolysis were determined in PBS buffer and 1% Triton X-100, respectively. For each concentration and control, the experiments were set in triplicate.

Circular Dichroism. CD experiments were carried out using a JASCO J-815 spectropolarimeter (Easton, USA) equipped with Peltier devices for temperature control. All of the spectra were obtained with a quartz cell of 0.2 mm path length. Spectra were recorded at a peptide concentration of 100 mM in different environments: water, phosphate buffer 10 mM, in 50% TFE, in the presence of SDS detergent (30 mM). The baseline-corrected spectra were smoothed, ellipticities were converted to mean residue molar ellipticities in degree $cm^2 \cdot d \cdot mol^{-1}$, and the helical content was estimated as previously described.[49]

NMR Experiments. All spectra were recorded on a Bruker Avance 500 spectrometer equipped with a 5 mm triple-resonance cryoprobe (PRISM, Rennes). One-dimensional spectra were first recorded at concentration around 1 mM for each peptide, dissolved in aqueous (90% H_2O, 10% D_2O) increasing SDS d-25 (Euriso-top) concentrations, and the pH was adjusted to 5.0 (until 200 mM SDS). Up to 50 mM SDS, variations in chemical shifts and line width narrowing could be observed, and then no change occurred at higher concentrations for all the peptides. The detergent concentrations were subsequently set at 50 mM for the further experiments. Homonuclear 2-D spectra DQF-COSY, TOCSY (MLEV), and NOESY were recorded in the phase-sensitive mode using the States-TPPI method as data matrices of 256 real (t_1) × 2048 (t_2) complex data points; 64 scans per t_1 increment with 1.5 s recovery delay and spectral width of 5341 Hz in both dimensions were used. The mixing times were 100 ms for TOCSY and 200 ms for the NOESY experiments. In addition, 2D heteronuclear spectra ^{13}C-HSQC and ^{13}C-HMBC were acquired to help to fully assign the naphthylalanyl side chains. Spectra were processed with Topspin (Bruker Biospin) or the NMRpipe/NMRdraw software package[50] and visualized with Topspin or NMRview[51] on a Linux station. The matrices were zero-filled to 1024 (t_1) × 2048 (t_2) points after apodization by shifted sine-square multiplication and linear prediction in the F1 domain. Chemical shifts were referenced to the solvent chemical shifts.

Structure Calculations. ^{1}H chemical shifts were assigned according to classical procedures.[52] NOE cross-peaks were integrated and assigned within the NMRView software.[48] Structure calculations were performed with ARIA 2.2.[53] Representation and quantitative analysis of the calculated structures were performed using MOLMOL[54] and PyMOL (Delano Scientific). The PROCHECK program[55] was used to assess the stereochemical quality of the structures. The calculations were initiated using the default parameters of ARIA and a nearly complete set of manually assigned NOE. The CNS[56] and ARIA topology and parameter files were modified to define the aza-β^3 residues based on the characteristic angles and distances in the previously published crystalline structures.[23−25] According to the N^{α} pyramidal inversion, the stereochemistry of the nitrogen bearing the side chain of the aza-β^3 residues is not fixed. The torsion angle φ was restrained to $-60 \pm 40°$ for $^3J_{HN-HA} < 6$ Hz. At the end of each run, violations and assignment proposed by ARIA were checked before starting a new run. This process was repeated until all the NOE were correctly assigned and no restraints were rejected. A last run of 60 structures was performed and refined in water; a set of 20 structures of lowest energies with no violation >0.3 Å were considered as representative of the peptide structure.

■ ASSOCIATED CONTENT

Ⓢ Supporting Information

Chemical shift of AD, AK, Aβ^3K, and K-Nal in presence of 50 mM SDS; structural statistics for the 20 models of AD, AK, Aβ^3K, K-2Nal7, and K-2Nal bound to SDS micelles; average torsion angles of the (*R*)- and (*S*)-Hydrazino turn and of the β-turn 2−5 and 5−8 for the Aβ^3K peptide. This material is available free of charge via the Internet at http://pubs.acs.org.

■ AUTHOR INFORMATION

Corresponding Author

*For M.B.-F.: phone, 33 (0)223236933; E-mail. michele.baudy-floch@univ-rennes1.fr. For A.B.: phone, 33 (0)223236561; E-mail, arnaud.bondon@univ-rennes1.fr.

Author Contributions

‖Contributed equally.

Notes

The authors declare no competing financial interest.

■ ACKNOWLEDGMENTS

We thank SERB Laboratories and Region Bretagne for their financial support and IFR 140 and Biogenouest for access to PRISM and Spectroscopies facilities. We are grateful to Prof. Françoise Vovelle for her helpful participation in the aza-β^3 residues description in CNS/ARIA parameter files. We gratefully acknowlegde Dr. Allan Cunningham for postediting the English style.

■ ABBREVIATIONS USED

AMPs antimicrobial peptides; SDS sodium dodecyl sulfate; NMR nuclear magnetic resonance; pI isoelectric point; na not active; SPPS solid-phase peptide synthesis; MIC minimal inhibitory concentration; MD molecular dynamics; NOESY nuclear Overhauser effect spectroscopy; ROESY rotating frame Overhauser spectroscopy; MS mass spectroscopy; HPLC high performance liquid chromatography; rmsd root-mean-standard deviation

■ REFERENCES

(1) Andreu, D.; Rivas, L. Animal antimicrobial peptides: an overview. *Biopolymers* **1998**, *47*, 415−433.

(2) Epand, R. M.; Vogel, H. J. Diversity of antimicrobial peptides and their mechanisms of action. *Biochim. Biophys. Acta* **1999**, *1462*, 11−28.

(3) Hancock, R. E.; Sahl, H. G. Antimicrobial and host-defense peptides as new anti-infective therapeutic strategies. *Nature Biotechnol.* **2006**, *24*, 1551−1557.

(4) Peschel, A.; Sahl, H. G. The co-evolution of host cationic antimicrobial peptides and microbial resistance. *Nature Rev. Microbiol.* **2006**, *4*, 529−536.

(5) Zasloff, M. Antimicrobial peptides of multicellular organisms. *Nature* **2002**, *415*, 389−395.

(6) Shai, Y. Mode of action of membrane active antimicrobial peptides. *Biopolymers* **2002**, *66*, 236−248.

(7) Brogden, K. A. Antimicrobial peptides: pore formers or metabolic inhibitors in bacteria? *Nature Rev. Microbiol.* **2005**, *3*, 238−250.

(8) Matsuzaki, K. Magainins as paradigm for the mode of action of pore forming polypeptides. *Biochim. Biophys. Acta* **1998**, *1376*, 391−400.

(9) Wu, M.; Maier, E.; Benz, R.; Hancock, R. E. Mechanism of interaction of different classes of cationic antimicrobial peptides with planar bilayers and with the cytoplasmic membrane of *Escherichia coli*. *Biochemistry* **1999**, *38*, 7235−7242.

(10) Bechinger, B.; Lohner, K. Detergent-like actions of linear amphipathic cationic antimicrobial peptides. *Biochim. Biophys. Acta* **2006**, *1758*, 1529−1539.
(11) Legrand, B.; Laurencin, M.; Sarkis, J.; Duval, E.; Mouret, L.; Hubert, J.-F.; Collen, M.; Vie, V.; Zatylny-Gaudin, C.; Henry, J.; Baudy-Floc'h, M.; Bondon, A. Structure and mechanism of action of a de novo antimicrobial detergent-like peptide. *Biochim. Biophys. Acta* **2011**, *1808*, 106−116.
(12) Arvidsson, P. I.; Ryder, N. S.; Weiss, H. M.; Gross, G.; Kretz, O.; Woessner, R.; Seebach, D. Antibiotic and hemolytic activity of a beta2/beta3 peptide capable of folding into a 12/10-helical secondary structure. *ChemBioChem* **2003**, *4*, 1345−1347.
(13) Porter, E. A.; Weisblum, B.; Gellman, S. H. Mimicry of host-defense peptides by unnatural oligomers: antimicrobial beta-peptides. *J. Am. Chem. Soc.* **2002**, *124*, 7324−7330.
(14) Schmitt, M. A.; Weisblum, B.; Gellman, S. H. Unexpected relationships between structure and function in alpha, beta-peptides: antimicrobial foldamers with heterogeneous backbones. *J. Am. Chem. Soc.* **2004**, *126*, 6848−6849.
(15) Chongsiriwatana, N. P.; Patch, J. A.; Czyzewski, A. M.; Dohm, M. T.; Ivankin, A.; Gidalevitz, D.; Zuckermann, R. N.; Barron, A. E. Peptoids that mimic the structure, function, and mechanism of helical antimicrobial peptides. *Proc. Natl. Acad. Sci. U.S.A.* **2008**, *105*, 2794−2799.
(16) Song, Y. M.; Park, Y.; Lim, S. S.; Yang, S. T.; Woo, E. R.; Park, I. S.; Lee, J. S.; Kim, J. I.; Hahm, K. S.; Kim, Y.; Shin, S. Y. Cell selectivity and mechanism of action of antimicrobial model peptides containing peptoid residues. *Biochemistry* **2005**, *44*, 12094−12106.
(17) Zhu, W. L.; Song, Y. M.; Park, Y.; Park, K. H.; Yang, S. T.; Kim, J. I.; Park, I. S.; Hahm, K. S.; Shin, S. Y. Substitution of the leucine zipper sequence in melittin with peptoid residues affects self-association, cell selectivity, and mode of action. *Biochim. Biophys. Acta* **2007**, *1768*, 1506−1517.
(18) Olsen, C. A.; Bonke, G.; Vedel, L.; Adsersen, A.; Witt, M.; Franzyk, H.; Jaroszewski, J. W. alpha-Peptide/beta-peptoid chimeras. *Org. Lett.* **2007**, *9*, 1549−1552.
(19) Shuey, S. W.; Delaney, W. J.; Shah, M. C.; Scialdone, M. A. Antimicrobial beta-peptoids by a block synthesis approach. *Bioorg. Med. Chem. Lett.* **2006**, *16*, 1245−1248.
(20) Violette, A.; Fournel, S.; Lamour, K.; Chaloin, O.; Frisch, B.; Briand, J. P.; Monteil, H.; Guichard, G. Mimicking helical antibacterial peptides with nonpeptidic folding oligomers. *Chem. Biol.* **2006**, *13*, 531−538.
(21) Dali, H.; Busnel, O.; Hoebeke, J.; Bi, L.; Decker, P.; Briand, J. P.; Baudy-Floc'h, M.; Muller, S. Heteroclitic properties of mixed alpha- and aza-β^3-peptides mimicking a supradominant CD4 T cell epitope presented by nucleosome. *Mol. Immunol.* **2007**, *44*, 3024−3036.
(22) Cheguillaume, A.; Salaün, A.; Sinbandhit, S.; Potel, M.; Gall, P.; Baudy-Floc'h, M.; Le Grel, P. Solution synthesis and characterization of hydrazinopeptoidic oligomers. *J. Org. Chem.* **2001**, *66*, 4923−4929.
(23) Le Grel, P.; Salaun, A.; Potel, M.; Le Grel, B.; Lassagne, F. Aza-β^3-cyclohexapeptides: pseudopeptidic macrocycles with interesting conformational and configurational properties slow pyramidal nitrogen inversion in 24-membered rings. *J. Org. Chem.* **2006**, *71*, 5638−5645.
(24) Salaun, A.; Potel, M.; Roisnel, T.; Gall, P.; Le Grel, P. Crystal structures of aza-β^3-peptides, a new class of foldamers relying on a framework of hydrazinoturns. *J. Org. Chem.* **2005**, *70*, 6499−6502.
(25) Salaun, A.; Mocquet, C.; Perochon, R.; Lecorgne, A.; Le Grel, B.; Potel, M.; Le Grel, P. Aza-β^3-cyclotetrapeptides. *J. Org. Chem.* **2008**, *73*, 8579−8582.
(26) Mocquet, C.; Salaun, A.; Claudon, P.; Le Grel, B.; Potel, M.; Guichard, G.; Jamart-Gregoire, B.; Le Grel, P. Aza-β^3-cyclopeptides: a new way of controlling nitrogen chirality. *J. Am. Chem. Soc.* **2009**, *131*, 14521−14525.
(27) Henry, J.; Zatylny, C.; Boucaud-Camou, E. Peptidergic control of egg-laying in the cephalopod *Sepia officinalis*: involvement of FMRFamide and FMRFamide-related peptides. *Peptides* **1999**, *20*, 1061−1070.
(28) Brogden, K. A.; Guthmiller, J. M.; Salzet, M.; Zasloff, M. The nervous system and innate immunity: the neuropeptide connection. *Nature Immunol.* **2005**, *6*, 558−564.
(29) Busnel, O.; Baudy-Floc'h, M. Preparation of new monomers aza-β^3-amino acids for solid-phase syntheses of aza-β^3-peptides. *Tetrahedron Lett.* **2007**, *48*, 5767−5770.
(30) Busnel, O.; Bi, L.; Baudy-Floc'h, M. Synthesis of Fmoc-protected aza-β^3-amino acids via reductive amination of glyoxylic acid. *Tetrahedron Lett.* **2005**, *46*, 7073−7075.
(31) Busnel, O.; Bi, L.; Dali, H.; Cheguillaume, A.; Chevance, S.; Bondon, A.; Muller, S.; Baudy-Floc'h, M. Solid-phase synthesis of "mixed" peptidomimetics using Fmoc-protected aza-β^3-amino acids and alpha-amino acids. *J. Org. Chem.* **2005**, *70*, 10701−10708.
(32) Laurencin, M.; Bauchat, P.; Baudy-Floc'h, M. Preparation of N^{β}-Fmoc-protected aza-β^3-amino acids with nonproteinogenic hydrophobic side chains for solid-phase syntheses of pseudopeptides. *Synthesis* **2009**, 1007−1013.
(33) Baudy-Floc'h, M.; Zatylny-Gaudin, C.; Henry, J.; Duval, E.; Laurencin, M. (SERB). French patent FR 07 09054 1808, 2007, pp 106−116.
(34) Dathe, M.; Nikolenko, H.; Klose, J.; Bienert, M. Cyclization increases the antimicrobial activity and selectivity of arginine- and tryptophan-containing hexapeptides. *Biochemistry* **2004**, *43*, 9140−9150.
(35) Wu, J. M.; Wei, S. Y.; Chen, H. L.; Weng, K. Y.; Cheng, H. T.; Cheng, J. W. Solution structure of a novel D-ss-naphthylalanine substituted peptide with potential antibacterial and antifungal activities. *Biopolymers* **2007**, *88*, 738−745.
(36) Haug, B. E.; Svendsen, J. S. The role of tryptophan in the antibacterial activity of a 15-residue bovine lactoferricin peptide. *J. Pept. Sci.* **2001**, *7*, 190−196.
(37) Hubert, F.; Noel, T.; Roch, P. A member of the arthropod defensin family from edible Mediterranean mussels (*Mytilus galloprovincialis*). *Eur. J. Biochem.* **1996**, *240*, 302−306.
(38) Sisido, M.; Egusa, S.; Imanishi, Y. One-Dimensional Aromatic Crystals in Solution 0.2. Synthesis, Conformation, and Spectroscopic Properties of Poly(L-2-Naphthylalanine). *J. Am. Chem. Soc.* **1983**, *105*, 4077−4082.
(39) Sisido, M.; Egusa, S.; Imanishi, Y. One-Dimensional Aromatic Crystal in Solution 0.1. Synthesis, Conformation, and Spectroscopic Properties of Poly(L-1-Naphthylalanine). *J. Am. Chem. Soc.* **1983**, *105*, 1041−1049.
(40) Dike, A.; Cowsik, S. M. Solution structure of amphibian tachykinin Uperolein bound to DPC micelles. *J. Struct. Biol.* **2006**, *156*, 442−452.
(41) Ivankin, A.; Livne, L.; Mor, A.; Caputo, G. A.; DeGrado, W. F.; Meron, M.; Lin, B.; Gidalevitz, D. Role of the Conformational Rigidity in the Design of Biomimetic Antimicrobial Compounds. *Angew. Chem., Int. Ed. Engl.* **2010**, *49*, 8462−8465.
(42) Arvidsson, P. I.; Ryder, N. S.; Weiss, H. M.; Hook, D. F.; Escalante, J.; Woessner, R.; Seebach, D. Exploring the Antibacterial and Hemolytic Activity of Shorter- and Longer-Chain β-, α,β-, and γ-Peptides, and of β-Peptides from β^2-3-Aza- and β^3-2-Methylidene-amino Acids Bearing Proteinogenic Side Chains—A Survey. *Chem. Biodiversity* **2005**, *2*, 401−420.
(43) Mowery, B. P.; Lindner, A. H.; Weisblum, B.; Stahl, S. S.; Gellman, S. H. Structure−Activity Relationships among Random Nylon-3 Copolymers That Mimic Antibacterial Host-Defense Peptides. *J. Am. Chem. Soc.* **2009**, *131*, 9735−9745.
(44) Goodballe, T.; Nilsson, L. L.; Petersen, P. D.; Jenssen, H. Antimicrobial β-Peptides and α-Peptoids. *Chem. Biol. Drug Des.* **2011**, *77*, 107−116.
(45) Schmitt, M. A.; Weisblum, B.; Gellman, S. H. Interplay among folding, sequence, and lipophilicity in the antibacterial and hemolytic activities of α/β-peptides. *J. Am. Chem. Soc.* **2007**, *129*, 417−428.
(46) Claudon, P.; Violette, A.; Lamour, K.; Decossas, M.; Fournel, S.; Heurtault, B.; Godet, J.; Mely, Y.; Jamart-Gregoire, B.; Averlant-Petit, M. C.; Briand, J. P.; Duportail, G.; Monteil, H.; Guichard, G. Consequences of Isostructural Main-Chain Modifications for the

Design of Antimicrobial Foldamers: Helical Mimics of Host-Defense Peptides Based on a Heterogeneous Amide/Urea Backbone. *Angew. Chem., Int. Ed. Engl.* **2010**, *49*, 333−336.
(47) Hetru, C.; Bulet, P. Strategies for the isolation and characterization of antimicrobial peptides of invertebrates. *Methods Mol. Biol.* **1997**, *78*, 35−49.
(48) Duval, E.; Zatylny, C.; Laurencin, M.; Baudy-Floc'h, M.; Henry, J. KKKKPLFGLFFGLF: a cationic peptide designed to exert antibacterial activity. *Peptides* **2009**, *30*, 1608−1612.
(49) Javadpour, M. M.; Juban, M. M.; Lo, W. C.; Bishop, S. M.; Alberty, J. B.; Cowell, S. M.; Becker, C. L.; McLaughlin, M. L. De novo antimicrobial peptides with low mammalian cell toxicity. *J. Med. Chem.* **1996**, *39*, 3107−3113.
(50) Delaglio, F.; Grzesiek, S.; Vuister, G. W.; Zhu, G.; Pfeifer, J.; Bax, A. NMRPipe: a multidimensional spectral processing system based on UNIX pipes. *J. Biomol. NMR* **1995**, *6*, 277−293.
(51) Johnson, B. A.; Blevins, R. NMRVIEW: a computer program for the visualization and analysis of NMR data. *J. Biomol. NMR* **1994**, *4*, 603−614.
(52) Wüthrich, K. *NMR of Proteins and Nucleic Acids*; Wiley-Interscience: New York, 1986.
(53) Linge, J. P.; O'Donoghue, S. I.; Nilges, M. Automated assignment of ambiguous nuclear overhauser effects with ARIA. *Methods Enzymol.* **2001**, *339*, 71−90.
(54) Koradi, R.; Billeter, M.; Wuthrich, K. MOLMOL: a program for display and analysis of macromolecular structures. *J. Mol. Graphics* **1996**, *14* (51−55), 29−32.
(55) Laskowski, R. A.; Rullmannn, J. A.; MacArthur, M. W.; Kaptein, R.; Thornton, J. M. AQUA and PROCHECK-NMR: programs for checking the quality of protein structures solved by NMR. *J. Biomol. NMR* **1996**, *8*, 477−486.
(56) Brunger, A. T.; Adams, P. D.; Clore, G. M.; DeLano, W. L.; Gros, P.; Grosse-Kunstleve, R. W.; Jiang, J. S.; Kuszewski, J.; Nilges, M.; Pannu, N. S.; Read, R. J.; Rice, L. M.; Simonson, T.; Warren, G. L. Crystallography & NMR system: a new software suite for macromolecular structure determination. *Acta Crystallogr., Sect. D: Biol. Crystallogr.* **1998**, *54*, 905−921.